

402 952

63-3-3

ASPHERIC OPTICAL ELEMENTS PROGRAM

INTERIM TECHNICAL REPORT NO. 15

FOR THE PERIOD 1 JANUARY 1963 TO 31 MARCH 1963

402952

ASTIA

CATALOGED BY

AD NO.

PREPARED BY

MARVIN MILLER AND MARVIN ROYSTON

CONTRACT AF 33(600) - 37199
DEPARTMENT OF THE AIR FORCE

MAY 8 1963

BELL & HOWELL COMPANY
7100 McCormick Road
Chicago 45, Illinois

ASPHERIC OPTICAL ELEMENTS PROGRAM

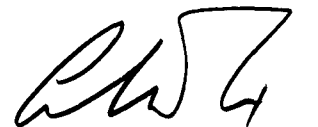
INTERIM TECHNICAL REPORT NO. 15

FOR THE PERIOD 1 JANUARY 1963 TO 31 MARCH 1963

OBJECT: To develop production manufacturing methods for extremely accurate aspheric lens surfaces.


Marvin Royston
Special Project Engineer

APPROVED BY:


Arthur Cox, Vice President
Photo Products Division

BELL & HOWELL COMPANY
7100 McCormick Road
Chicago 45, Illinois

"The work reported in this document has been made possible through the support and sponsorship extended by the Manufacturing Methods Branch, Air Material Command. It is published for technical information only and does not necessarily represent recommendations or conclusions of the sponsoring agency."

TABLE OF CONTENTS

	Page
PURPOSE	1
ABSTRACT	2
LOW FREQUENCY, HIGH DENSITY PULSE TECHNIQUES . .	5
Magnetic Drums for In-Contact Heads	8
Flux Rate Sensitive Transducers	11
STABLE FLUX RATE SENSITIVE READ HEAD AMPLIFIER .	15
General Discussion	15
Technical Development and Design	21
Preamplifier	21
Resolution Amplifier	39
Phase-Inverter Amplifier	42
Switching Amplifier	46
Comparator Amplifier	49
Figures 1 through 9	52
LENS DESIGN	61
RECOMMENDATIONS	63
DISTRIBUTION LIST	

PURPOSE: There is a need to investigate and develop production manufacturing methods for aspheric lens surfaces. In order to achieve the ever-rising quality requirements for photographic objectives, it has become necessary to use aspheric surfaces in the design of lens systems. It has been established that such surfaces will allow for greatly increased quality and at the same time for a reduction in size and weight of the optical system.

The purpose of this contract is to develop equipment and methods for large quantity production of precise aspheric optical elements. Evaluation of the repeated accuracy of manufacturing methods will be accomplished by subjecting the lenses made to careful inspection and by employing them in photographic objectives.

WORK COMPLETED 82.6% of ENTIRE CONTRACT
100% of PHASE I
100% of PHASE II
71% of PHASE III

(BASED ON CONTRACT SPECIFICATIONS)

ABSTRACT: The work covered by this report represents the period which just precedes the start of integration of the entire control complex with the machine tool itself. This is a period which is significant in that many problems present a choice of multiple solutions with an extensive range of apparent reliability and cost implications. It has been necessary to resolve many of the major problems in this category in order to be able to continue the project unabatedly.

Early in this program it was felt that a general policy of "over-design" should be adopted, and this approach was stated in Interim Reports 2 and 3. Such a policy was concluded in view of certain basic unknowns in the areas of the diamond tool and its behavior relative to various rates of slope change, Interim Technical Report No. 11, Pages 4 to 10, and variables in the work spindle and physical variations between the work and the tool due to changes in thrust load and ambient temperatures.

It was felt that everything possible should be done to make sure that the relative positions of the work and tool carriages are in their calculated positions, increment by increment. Any deviations of the desired posi-

tions of the carriages would certainly mask errors due to misbehavior of the tool, and it would be virtually impossible to evaluate and correct such errors.

A study of the factors which determine the accuracy of the relative position of the carriages revealed that the weakest link in the control chain was that of the reliability of the placement of command pulses on the B drum and the ability to retrieve these pulses without error. This, of course, requires the same reliability from pulses placed on all magnetic drums involved in both the recording of the B1 command pulses as well as the response pulses at the C drum during the machining of glass.

Therefore, a program was instituted early in December of 1962 to improve the magnetic drum itself, to optimize the electrical impedance and gap widths of the read and write heads, and to greatly improve the amplifiers for the velocity sensitive read heads employed for the A, B1, and B2 readout. Improvement of the magnetic drum and the write heads will also result in further improvement of the C pulses where flux sensitive read heads are being used. This phase of the program has now yielded to the search for the means of improving pulsing techniques for

the low surface speed and high packing density required of this system. Therefore, this report will deal mainly with the details of the means by which the resulting reliability of magnetic pulsing was accomplished.

Parallel with this activity, the new translator has been nearly completed, and many other areas of work involving the main control panel and interconnecting cabling has proceeded routinely.

Two errors were made in Table I, Page 15 of Interim Technical Report Number 14 and should be corrected as follows:

- 1) In the third line, change Number 3548 to 3584.
- 2) In the fifth line, change the Number 366 to 336.

All of the other numbers in the table are correct.

LOW FREQUENCY, HIGH DENSITY PULSE TECHNIQUES

At the inception of the finally adopted numerical control system, it was recognized that the major problem regarding pulse recording and retrieval was presented at the Y axis. Since the allowable deviations at the Y axis are about $1/4$ that of the transverse motion at the X axis, the retrieved information from the Y axis must be in the order of four times that for equal amounts of carriage travel at the X axis. Further, the information at the Y axis must be retrieved at speeds down to and including zero. This problem was adequately solved with the use of modulator type flux sensitive read heads and was thoroughly explored in Interim Report Number 6.

At that time it was planned that flux sensitive heads would also be employed for the X axis pulses due to the low speeds involved. However, preliminary experiments with the simpler flux rate sensitive read heads, or velocity heads, have revealed unexpectedly good ratios of apparent signal-to-noise ratios at surface speeds as low as $1/10$ of an inch per second. Whereas the output of the read head is relatively low at a surface speed of $1/10$ inches per second, the intrinsic noise from the magnetic coating is also relatively low for the same reason. Also noteworthy is the low maximum pulse rate required at the X axis, which is 336 pulses per second, Interim

Technical Report Number 14, Page 15. Therefore a low-pass filter can be disposed at the output of the A and B read head amplifiers eliminating spurious noises above the 336 pulse rate, regardless of where they may be injected in the low level circuitry. (It should be noted that the filter is placed in the circuit before the four-times multiplier for the A pulses.)

Since the lowest surface speed of the recording medium required of drums at the X axis is substantially higher than the 1/10 inches per second, which showed promise in the preliminary experiments, further work was done with velocity heads leading to the adopting of this type of head for the A, B1, and B2 pulses at the X axis.

It should be pointed out that no one working in the fields where pulse techniques are extensively used could predict what results to expect with the use of velocity read heads at such low surface speeds. Therefore, we proceeded with caution since these parameters seemingly have not been explored.

As a starting point, we made use of experimental drums coated with 3M-RD3010 dispersion over a .015 inch undercoat of rubber on an aluminum drum, Interim Technical Report Number 6. The drum was transported by a dividing head type of turntable. A 100 mh head with a 160 micro-inch gap was employed for both the write and read

modes. For the readout a conventional solid state audio preamplifier which contained a bass boost of 6 db per octave below 500 cps was used. At a packing density of 233 cycles (466 NRZ reversals) per inch and a reading speed of 1/10 inches per second, a signal-to-noise ratio of 45 db was obtained. The noise was 60 cycles, seemingly picked up by the input coax rather than by the head. The source of the interference was a shaded pole motor used to drive the turntable and was positioned about 16 inches from the head and coax lead.

Direct voltage measurements at the velocity head with a conventional VTVM, when reading pre-recorded pulses representing the packing density to be used for the A drum, and at a speed of 1/10 inches per second, proved ambiguous when compared with the output voltages of an amplifier of known gain. It was quickly realized that special equipment must be employed to obtain true readings at levels in the order of 15 to 50 micro-volts appearing at the output of the velocity head under these conditions. Any unbalanced condition and any condition permitting even a slight ground loop at these levels will result in the acquisition of untenable spurious noise. It was this observation which led to the development of special d.c., pushpull amplifiers and other special circuitry, described in the section "STABLE FLUX RATE SENSITIVE READ HEAD AMPLIFIER". This observation also led to a decision to further optimize

the magnetic drums and the write and read heads which will now be described. All three problem areas were tackled simultaneously.

Magnetic Drums for In-Contact Heads

There was a factor, in addition to those already mentioned, which dictated the necessity for further improvement of the magnetic drum. Up to this time the only drum which gave sufficiently stable read amplitude levels was one which employed an undercoat of rubber, .015 inches thick. Drum coatings without the use of resilient backings yielded an output signal which averaged 5 d.b. lower in level and worse; during a single turn of the drum, the signal level varied by 10 or 12 d.b. with occasional dropouts. However, two serious problems with the rubber backed coating existed. 1) It was feared that cold flow of the rubber might displace relative portions of the pulses annularly within the 360 degree track of pulses at the A and C drums. This could be particularly serious at the C drum, since a second head is disposed by a 90 degree phase relationship in order to obtain a multiplication of the C pulses by a factor of two. Any annular shift of pulses in the vicinity of one head relative to those in the vicinity of the second head would result in the loss of pulses if the relative shift approached 90 degrees. 2) With the two years which have passed since the rubber undercoated drum was fabricated, the magnetic coating developed cracks cross-wise to the recorded track which caused dropouts.

1

In December of 1962 Mr. George Cheney, Research Supervisor of Bryant Computer Products of Walled Lake, Michigan, indicated the willingness of his company to work on the problem. On 26 December 1962 Mr. Royston visited Bryant Computer Products in Walled Lake. It was learned that Bryant is currently using a new magnetic dispersion on their "Magnetic File" systems.

The new emulsion contains magnetic particles which are substantially square in physical shape. This results in microscopic magnetic particles which are shorter in maximum length and which allow higher packing densities. Actually, since no method has been evolved for pre-orienting magnetic particles on magnetic drums, the more pronounced improvement might be in the area of greater amplitude stability from the recorded pulses. Secondly, the new emulsion exhibits somewhat higher coercive and retentivity forces which could result in higher amplitude pulses under certain circumstances and in less deterioration of the signal under the influence of possible small amounts of inadvertent external magnetic flux fields.

Two blank drums were given to Mr. Cheney for the application of experimental magnetic coatings. On one, Bryant's LS200, emulsion was placed directly onto the base metal. On the second drum the same emulsion was used but an undercoat of acrylic, .010 inches

thick, was applied in order to give a small amount of compliance in the backing.

With the use of optimized heads, to be described in the following sub-section, the two drums were tested and evaluated. Readout from pulses recorded on the drum where the emulsion was placed directly onto the base metal gave an output level which was about 4 d.b. lower than that obtained from the older rubber backed drum. But most important, the signal variation from the Bryant drum varied only one d.b. during one or more turns of the drum. Even though the output level is lower than the previous rubber backed drum, it is higher than previous drums where the other dispersion was placed directly on the base metal and is very adequate for this application.

The second drum with the acrylic backing gave excellent results with an increased read level of about 4 d.b. However, after a period of use, the surface showed signs of abrasion. Therefore, any thought of employing resilient backings has now been abandoned, particularly in view of the uniform performance obtained from the other drum from Bryant.

Two more variables in respect to drum coatings will be tried before coating of the final drums will be approved. The first two experimental drums from Bryant contained magnetic coatings which were

.008 inches thick, which is .003 to .004 thicker than normal. Also, since our application requires heads-in-contact, Bryant will supply their LS216 emulsion which contains a lubricant but is otherwise identical to their LS200 and will maintain a coating thickness of .0004 to .0005 inches.

One of the implications of the excellent results obtained with the Bryant drums for heads-in-contact use, is that their preparation of the metal surface and uniformity of their dispersion is superior, resulting in good and uniform intimacy between the write-read heads and the magnetic surface.

Flux Rate Sensitive Transducers

The original experiments in low surface speed/high density pulsing at Bell & Howell were performed during Phase II of this contract and reported in Interim Technical Report Number 6. During this period of time, recording heads designed for sound recording were employed as write heads. Heads containing .001 and .00025 gaps were tried. No attempt was made to determine optimum parameters as to impedance and gap width for either the write or read heads.

In order to obtain optimum performance at the X axis with the use of velocity heads, it was decided that the proper parameters should be obtained for both the write and read heads. It was further known that any improved performance due to optimization of the

write head would certainly benefit the pulse technique for flux sensitive readout as well.

The write head driver amplifier was altered to allow a much faster rise time such that the rise time could then be progressively adjusted downward in order to obtain the optimum rise time for any given condition of packing density and surface speed. With this extended rise time capability, new write heads were built at Bell & Howell, making use of laminated pole shoes and much lower impedance windings to make sure the write head would respond to the faster rise time. Also progressively shorter gaps for the write heads were tried.

For both write and read heads, parameters of the transducer were changed, one at a time. For each change in impedance and gap values of the write head, the external environmental parameters were varied to obtain the maximum recorded pulse level by progressively varying the packing density, the NRZ rise time, the surface speed, and the record current. For each of these conditions, the readout level was measured at surface speeds of 0.1 ips and 0.8 ips which is beyond the low and high limits to be encountered in the aspheric machine for the velocity read heads. The above tests were repeated for each change in impedance and gap value of the read head.

The results of these experiments were very enlightening and, in certain areas, surprising, mainly in that some of the parameter variations did not produce the expected "spread" in measurable results. This points up our conclusion that the factors affecting the actual amplitude of densely packed pulses are complex indeed. As an example of this, it was found that under one set of circumstances where the packing density was varied over wide ranges, with each packing density value optimized from the standpoints of record current and read gap value, the maximum readout amplitude did not occur at the lowest packing density as was expected. Progressing upward from a density as low as ten cycles per inch, the amplitude started to rise near the peak which occurred at about 200 cycles (400 NRZ reversals) per inch, above which it progressively dropped as expected. Since the write head resonance was in a frequency range in the order of 100 times that represented by the rise time used for each pulse, and since the read head resonance was in the order of 1000 times the frequency at which the pulses were retrieved at the 200 cycle density point, resonance can be ruled out as the cause.

A loss of amplitude at the higher packing densities during the recording process is expected due to self erasure. But the only explanation we have for a peak occurring at 200 cycles per inch, when compared to much lower packing densities, is that the flux

spread from the write gap, which accounts for self erasure at high packing densities, must have a reinforcing action on the adjacent pulse just previously recorded which is at just the right distance from the pulse being written at the moment to receive a pulse steepening effect.

Since the A and C drums are pre-recorded on a dividing head type of turntable with synchronized pulses, which are independent of a time basis, the surface speed and other parameters can be selected to take advantage of the above phenomena.

Many pages of data have been recorded as a result of the above experiments. However, it is believed that no useful purpose would be served by issuing such information before the final data have been obtained from the drums now being processed with Bryant's ES216 emulsion. In the meantime, it can be stated that the pulsing techniques already developed indicate a high level of reliability.

STABLE FLUX RATE SENSITIVE READ HEAD AMPLIFIER

General Discussion

The read amplifiers are high quality amplifiers designed for low level operation as mentioned in the interim technical report Numbers 10 and 13. Parameters for this application must include characteristics such as very low noise, high gain, and good stability. Other important considerations consist of d.c. operation and broad dynamic input signal ranges. The common mode rejection properties of external signals must also be good. The signal-to-noise threshold adjustment for reducing the dead-zone in the output switching circuits must be very stable and accurate.

With this in mind, a step was taken to review the overall requirements of this amplifier. Then a careful investigation was made of both the proper design approach to use and the method of packaging the design for the greatest signal-to-noise ratio. As a result of the investigation, the amplifier has been divided into five sections:

1. Preamplifier.
2. Resolution amplifier.
3. Phase-inverter amplifier.
4. Switching amplifier.
5. Comparator amplifier.

Each section is packaged on individual plug-in type modules. The preamplifier as shown schematically in Figure 2 is located adjacent to the velocity heads on both A disc and B drum. This was done to improve the signal-to-noise ratio by reducing the lead length from the velocity head to the first amplifier stage. With this technique, the read signal is first amplified several thousand times by a d.c. differential amplifier with low impedance push-pull balanced output stages for driving a coaxial transmission line. From this point, the read signal is carried to the main section of the amplifier with sufficient amplitude to overcome any external interference signals that may be detected in the coaxial line.

The output of the preamplifier is then fed into the resolution amplifier module, Figure 3, where the push-pull signal is reduced to single ended operation. This is accomplished by mixing the differential signal of the preamplifier at the collector of transistor, Q9 of Figure 3. The output signal of transistor Q9, which now combines both sides of the push-pull, is further amplified by this section. The frequency response of both the preamplifier and resolution amplifier is from d.c. to 200 cycles per second with an overall gain of 30,000 times.

The next section to consider is the phase inverter amplifier module, Figure 4, where additional functions are incorporated besides amplification. The first significant difference we find is that

a.c. coupling is employed. Somewhere along the chain of amplification stages, we must isolate the d.c. drift component. This becomes mandatory from both a stability and reliability standpoint.

Since the frequency response requirement is all in the lower range of the spectrum, a minimum number of coupling capacitors are used. The first two common emitter amplifiers contain the only a.c. coupling networks in the entire read amplifier design. The purpose of this was to reduce any blocking effect resulting from high amplitude transients or signals. The major problem with the coupling capacitors used with transistors is that the capacitor value itself must be quite high with relative low input impedance of the transistor. Since both the frequency response requirement is low and the capacitor value high, the recovery time or discharge time of the capacitor is quite important. In order to reduce this discharge time, a minimum number was used in the design.

The remainder of the capacitors required in the system are for applications listed below:

1. B supply filtering.
2. High frequency response control.
3. Phase shift correction.
4. Signal rise time control.
5. Signal isolation.
6. Differential networks.
7. Pulse coupling.

The phase inverter amplifier as previously mentioned also performs other functions. Since NRZ recording techniques are used in this equipment, the inverter amplifier is used to invert the trailing edge of the differentiated waveform from the velocity head. This essentially doubles the number of pulse-bits per inch and increases the control system resolution.

The other functions of this section are related to the amplifier noise-threshold at various signal levels. This is a separate function from the actual system threshold control used in the monostable multivibrator. All the stages from the paraphase amplifier Q17 through the last stage Q22 of Figure 4 are d.c. coupled.

The next section to consider is the switching amplifier module of Figure 5. This section is also d.c. coupled from the first amplifier stage Q23 through the driver stage Q25. From the driver stage the signal passes through a steering diode and diode gate network on to the monostable multivibrator. The multivibrator Q26 and Q27 of Figure 5 generates a pulse at a fixed time duration and amplitude for controlling the necessary logic circuits in both the machine control and translator system. The remaining transistors Q28 and Q29 are emitter follower type amplifiers to provide the proper low impedance for driving the coaxial transmission line and logic gates.

1

Included in this module is a frequency meter network and amplifier stage Q30 for driving a small meter. This meter is mounted on the module plug-in case for monitoring the output pulses from the multivibrator. The pulse rate can, therefore, be checked quite easily by this indicator. The most important feature is directly related to servicing the equipment when failure of both components and cables occur.

The next and last function of the read amplifier is the comparator amplifier module shown in Figure 6. This circuit function is rather unusual in both its application and performance. The main object of this section is to supply the gate control voltage to the diode blocking gate. This in turn controls the incoming pulse signal from the output amplifier Q25 to the monostable multivibrator Q26 and Q27 of Figure 5.

The comparator detector network consists of two relaxation oscillators controlled by a differential amplifier Q32 and Q35. The read system threshold adjustment for triggering the output multivibrator is accomplished at potentiometer R42. This adjustment controls the system sensitivity and determines the exact level at which the switching amplifier will operate. Additional function of the comparator amplifier section includes a unique application of a solid state filter especially designed for the comparator control system. Further description of this and preceding modules

will be given later in this report.

A block diagram illustrating the operation of the read amplifier system is shown in Figure 1.

Technical Development and Design

Preamplifier

The preamplifier is the heart of the entire read amplifier design. It determines both the minimum signal level and maximum common mode rejection capability of the system. It is this circuit function that permits reliable operation of equipment employing velocity heads operating at very low speeds.

The internal noise of the first transistor stage is in the vicinity of .06 microvolts. Consequently, a 6 microvolt signal would provide a signal-to-noise ratio of 100:1 or 40 d.b. This would be fine if the first stage noise of Q₁ and Q₂ was the only mode of interference. Other sources such as 60 cycles ground current and transient voltages developed from electric motor or other control devices are major problem areas to consider. With the addition of all the external sources of noise, the system capability is degraded and overall performance is lowered. In order to minimize this condition, a d.c. differential amplifier was designed with dual negative feedback loops. This combination was chosen for two very important reasons. The differential design was employed because of the common mode rejection capability, while the direct coupling technique was required to prevent differentiation of the input signal and to reduce temporary blocking caused by the high capacitor coupling values. Another problem

that arises with the coupling capacitors is related to the frequency response. Since there is a low frequency response requirement but not as low as d.c., a high value capacitor is mandatory. This is primarily due to both the low input impedance of the transistor and the equivalent sign wave frequency response of 30 cycles per second. This equivalent response is at the very low packing density rate. Although the velocity head output waveform voltage is a differentiated form of the recorded square wave, the input capacitor value required to prevent further differentiating becomes astronomical. It is this phenomena, the second order differentiation that becomes the major reason for using the direct coupled design in the preamplifier.

Should the waveform be a conventional sine wave as it is at the higher packing densities, the only detriment to the system performance would be in terms of lower sensitivity caused by the increased capacitive reactance X_C . However, since the signal waveform is a square wave at the lower packing densities, the velocity head output voltage $E_o = \frac{N}{10^8} \frac{d\phi}{dt}$ becomes the first derivative of the NRZ recorded square wave. This is shown in Figure 7A - 1a and 7A - 2a. Now if a coupling capacitor is used on the input of the amplifier, the combination of both the low input impedance H_{11} of the transistor and the capacitive reactance X_C will again cause differentiation. Consequently the amplifier

encountered in computing a linear function with the conventional differential formulas. However, this is not true with a step function that contains a large quantity of harmonics. Other approaches must be used that express the complex variables and transient characteristics encountered in a square wave. To do this we must refer to the fourier integral that provides the proper transform for expressing this function.

Before expanding on the specific system problem, a few general remarks will be made. The fourier series as applied to phase angles of harmonic components can be expressed as an independent variable. This variable is associated with a definite period of time and is related as $f(t) = f(t+kT)$. The period of this function as expressed by the relationship $f(t)$ is known as the fundamental period T . The reciprocal of T is the fundamental frequency $f = \frac{1}{T}$.

The angular or radian frequency ω is $= 2\pi f = \frac{2\pi}{T}$. The fourier series representing the periodic function $f(t)$ can be expressed as $f(t) = \frac{a_0}{2} + a_1 \cos \omega t + a_2 \cos 2\omega t + \dots$
 $+ b_1 \sin \omega t + b_2 \sin 2\omega t + \dots$

and the phase angle of the harmonic components can be written as a sum of sine or cosine terms. The term having the fundamental angular frequency is commonly called the fundamental component of the periodic function $f(t)$. The periodic function can then be

expressed in terms of angular frequency as

$$f(t) = \frac{C_0}{2} + C_1 \cos(\omega t + \phi_1) + C_2 \cos(2\omega t + \phi_2) + \dots$$

The remaining terms, whose frequencies are integer multiples of the fundamental, are known as harmonics. Because of the periodic nature of the function $f(t)$, it is usually possible to select the origin for the independent variable t at any point.

There are quite a number of methods to establish a fourier series to represent a function that can be defined over a finite region. However, for practical reasons, we will limit the expansion to a minimum number of terms. In the case of a square wave we have the expression

$$\alpha_n = \frac{\omega}{2\pi} \left[-\int_{-\pi/\omega}^0 e^{-jn\omega t} dt + \int_0^{\pi/\omega} e^{-jn\omega t} dt \right]$$

In general, one can regard the coefficient α_n as a function of the variable $n\omega$, which is the angular frequency of the harmonic component of order n . The function $\alpha(n\omega)$ is often referred to as the fourier transform of $f(t)$ and the latter as the inverse transform of $\alpha(n\omega)$.

With the above in mind, we are acquainted with the periodic function of $f(t)$ and will, therefore, apply this period function with the fourier integral. The fourier integral brings us into the main subject of interest. It is this technique that satisfactorily provides an answer to the second derivative a.c. coupling problem.

The linear superposition of a group of discrete, uniformly spaced, frequency components causes an interference pattern of a periodic nature. This interference pattern assumes a transient character when the frequencies in the same group are continuously distributed. These frequencies are often referred to as the continuous spectrum and should be thought of as a line spectrum in which the spacing of the lines is allowed to approach zero. The transient character of the resulting time function can then be thought of as a limiting form of a periodic function for which the period has become infinite. It is evident that the two limiting processes are consistent from the fact that the line spacing in the spectrum of a periodic function equals its fundamental frequency. Also the period (reciprocal of the spacing of lines) is equal to the line density expressed as the number of lines per cycles per second. And as this period is permitted to increase, the line density increases, so that the final spectrum becomes a continuous one and the function never repeats. As a result, it becomes a transient function. The fourier integrals of both periodic function $f(t)$ and the fundamental angular frequency are given as follows:

$$f(t) = \int_{-\infty}^{\infty} g(\omega) d\omega e^{j\omega t}$$

$$g(\omega) = \frac{1}{2\pi} \int_{-\infty}^{\infty} f(t) dt e^{-j\omega t}$$

The foregoing material furnishes the necessary ground work for familiarizing one with the periodic function $f(t)$ and the fundamental angular frequency $g(\omega)$. The next and last phase con-

siders the error function and its sequence of singularity functions. The sequence of singularity functions and their transforms may be derived through applying suitable limiting processes to a variety of properly chosen functions. The one of interest for this application is the error function.

The error function has the form of $f(t) = e^{-at^2}$ and the transform of error function is given by $g(\omega) = \frac{1}{\sqrt{\pi}} \int_0^{\infty} e^{-at^2} \cos \omega t \, dt$. After integrating we have $g(\omega) = \frac{e^{-\omega^2/4a}}{2\sqrt{\pi a}}$

Now if we let $a = \frac{\pi}{\alpha}$ and then multiply the resulting time function and its transform by the factor $\frac{1}{\sqrt{\alpha}}$, the time function becomes

$$f(t) = \frac{e^{-\pi t^2/\alpha}}{\sqrt{\alpha}} \quad \text{and its transform}$$

$$g(\omega) = \frac{e^{-\alpha \omega^2/4\pi}}{2\pi}$$

The time function for this is shown in Figure 7B - 1b. This is the same type of waveform output produced from the velocity head at the low packing densities. From Figure 7B - 1a, we find that as α becomes smaller, the curve for $f(t)$ becomes greater in amplitude and less in time duration. Also if the limit of α approaches zero, the waveform then takes on the character of the original square wave found on the recording.

Now if we want to know what the waveform characteristic is after using capacitive coupling into the first transistor stage, we can

take the waveform of Figure 7B - 1a and differentiate the function of $f(t)$ and its corresponding transform $g(\omega)$. The expressions now become as follows:

$$f'(t) \quad \frac{df}{dt} = \frac{2\pi t}{\alpha^{3/2}} e^{-\pi t^2/\alpha}$$

$$g(\omega) \quad g'(\omega) = \frac{d\omega}{2\pi} e^{-\alpha \omega^2/4\pi}$$

The first derivative of waveform Figure 7B - 1b is shown in Figure 7B - 2b. This is actually the second derivative mentioned earlier, concerning the original recorded square wave.

Just for interest sake in network design technology, the differentiated waveform of Figure 7B - 2b is shown in the next figure of 7B - 3b.

The expression for this is

$$\frac{d^2f}{dt^2} = \frac{2\pi(2\pi t^2 - \alpha)}{\alpha^{5/2}} e^{-\pi t^2/\alpha}$$

Now from all the waveforms shown in Figure 7B and the Fourier series equations, a number of system characteristics can be performed. The first considers the fundamental frequency. This frequency waveform is available directly from the velocity head, Figure 7B - 1b. The next waveform, Figure 7B - 2b, is the first derivative and can be used in the design of a pulse doubling network. This is where the actual error is introduced, as described earlier in the report. With this phenomena of second order differentiation, twice as many output pulses will occur.

Consequently, an approach was taken to eliminate this effect. This was accomplished by employing direct coupling in the pre-amplifier design.

The last waveform, as shown in Figure 7B - 3b, is the second derivative of 7B - 1b, or the third derivative of the recorded square wave. This waveform indicates that three times as many pulses will be generated if care is not observed in the overall system design.

The actual differential design will now be considered and the related problems associated with it. In the past it has been very difficult to design stable d.c. amplifiers employing transistors. This was primarily due to the wide variations in transistor parameters with changes in ambient temperatures. The important parameters to consider are listed as follows:

1. Base to emitter voltage V_{BE} .
2. Collector to base leakage current IC_{BO} .
3. Current gain factor h_{FE} .

Since this amplifier cannot be a.c. coupled, at least until the proper impedance transfers are made, it is apparent that a minute shift in the bias operating point cannot be distinguished from a drift in the input voltage. Therefore, it is mandatory that the operating point and current gain factor h_{fe} be stable with changes

in temperature.

Recent significant advances in transistor technology in passivated junction surfaces have resulted in the base to emitter voltage V_{BE} of two transistors to become more identical. This contributes to superior performance of two devices that have been passivated on the same substrate and mounted inside the same transistor envelope. The stability of an amplifier can consequently be increased by an order of magnitude. This technique decreases thermal differentials that are normally encountered in two dimensional separated junctions. Therefore, drift in a d.c. amplifier originates almost exclusively in the differential input transistors, and arises primarily because of aging and temperature changes in the three previously mentioned parameters, V_{BE} , I_{CBO} , and h_{FE} . Silicon transistors that have leakage currents I_{CBO} of one millimicroamp. ($1nA$) at $25^{\circ}C$ have effectively eliminated this source of drift. The major problem source is in the base to emitter voltage V_{BE} . This junction voltage is stable with time but exhibits marked temperature dependence by decreasing at approximately 2mv. for every degree centigrade rise. The differential design approach tends to minimize this effect since the base to emitter voltage drops are in series opposition. If we now consider this phenomenon to be reduced and furthermore consider two transistors exactly matched but in separate packages, the equivalent input drift of 20 microvolts will result for every

.01°C temperature differential between the two transistors. This temperature differential has now been alleviated since the development of a dual transistor that is passivated on one common substrate and mounted inside the same TO-5 package. This contributes to improved stability and reliability of equipment employing such devices in the design of solid state differential amplifiers.

The design of the preamplifier includes techniques of using a dual transistor hermetically sealed in one enclosure. For both practical and technical reasons, we have selected the Fairchild 2N2223 transistor. This transistor provides a maximum differential base voltage V_{BE} of 15 mv at .1 ma. between the two junctions. Other transistors, such as the 2N2223A, provide a 5 mv differential voltage. This is better by a factor of three times but is not necessary for this application. This is primarily due to the fact that d.c. voltage amplification is required only to prevent differentiation of the input signal.

The Fairchild Company states that these devices will maintain the same performance and reliability as the planar types available for applications demanding high performance.

Another approach to consider is the chopper method for low frequency applications. Mechanical choppers have been widely used to convert d.c. voltages into a.c. This method suffers from the inherent very low frequency limitation and the reliability of the

mechanical component. The mechanical function can be removed by using transistor choppers. This approach appears to be more reliable but adds to the complexity of the design.

The use of direct coupled amplifiers without chopping is quite attractive from the standpoint of reduction in design complications. This approach is better for the read amplifier system, since it has the advantage of reducing the noise, size, weight, cost, and power requirements. Furthermore, it offers higher operating frequency capabilities.

The advantage of size is an attribute of prime importance to this system since it is quite important to locate physically the preamplifier as close to the read velocity head as possible. As mentioned earlier in the general discussion section, the reason for locating the preamplifier close to the read head was to reduce the coaxial lead length of the cable to a minimum. The prime objective was to reduce the possibility of transient noise that may be picked up in the cable.

In the design of the preamplifier, extreme care must be observed to stabilize and establish the proper d.c. operating point. A brief description of the equivalent input circuit and related equations are given for the design of differential amplifier. The input transistors Q1 and Q2 of Figure 2 are shown separately in

Figure 8. The output function is given of the two output voltages e_{1out} and e_{2out} at the collector of Q1 and Q2. Output of Q1 is given as follows:

$$e_{1out} = \frac{R_L}{R_S(h_{FE1} + h_{FE2}) + R_E} \left[(e_2 - e_1) + \right.$$

$$\left. \Delta V_{BE} + R_S \Delta I_{CO} \frac{R_{E2}}{R_{EE}} (e_1 + V_{BE1} - R_S I_{CO1} - V_{EE}) \right] + I_{CO1} R_L - V_{CC}$$

A similar expression is written for the output voltage of transistor Q2. The term relating to VEE may be small if R_{EE} is sufficiently large. This can easily be accomplished by using the impedance transfer gain of a transistor that is operated in a constant current mode. The constant current transistor QA and its network are shown in Figure 2.

The primary parameters responsible for drift in the amplifier as mentioned earlier are the thermal effects on the emitter to base voltage V_{EB} , current gain h_{fe} , and collector to base leakage I_{CBO} . From the equation $e_{2out} - e_{1out}$, it can be seen that if R_b approaches 0, the effects of h_{fe} variations are small. This condition, however, tends to restrict operations of the amplifier to applications having very low source impedance. It is possible to improve this by operating at a collector current as low as possible. Again, there is a compromise since the output impedance rises with the lower collector currents. The complete differential voltage e_{1out} and e_{2out} is:

$$e_{1OUT} - e_{2OUT} = \frac{2R_L}{R_S \left(\frac{hFE_1 + hFE_2}{hFE_1 hFE_2} \right) + R_E} \left[(e_2 - e_1) + \right. \\ \left. (\Delta V_{BE} + R_S \Delta I_{CO}) - (R_E I_{CO2} + V_{EE} - V_{BE2} - e_2) \left(\frac{R_{E1} - R_{E2}}{2 R_{EE}} \right) \right] + R_L \Delta I_{CO}$$

The most difficult problem to overcome is the matching of the magnitude and temperature coefficient of the emitter to base voltages V_{EB} . Both of the quantities are a function of the current gain, emitter current, doping densities of the emitter and base junction, as well as the relative magnitudes of diffusion and space-charge region recombination currents.

The above matching has been accomplished as closely as economical reasons are concerned and drift effects minimized as much as the state of the art permits.

Another important consideration in low level amplifiers is noise. The transistor noise decreases at low values of current until a point is reached of approaching the collector leakage current. Also, the current gain factor hfe must remain high enough for a good signal-to-noise ratio. In order to accomplish this, a transistor must have excellent current gain properties at low operating currents.

The amplitude spectrum of transistor noise is shown in Figure 9. At low frequencies the noise is predominantly flicker noise,

which varies approximately inversely with frequency $\frac{1}{f}$. It has a noise source from both the surface and leakage components with a slope of 3 d.b. per octave. Surface noise is caused by fluctuations of energy levels at the junction surfaces which modulate the junction resistances. This type of noise is very current dependent, whereas the leakage noise is caused by the leakage current across the junction. The leakage noise is therefore dependent upon bias voltages. At voltages less than 10 volts the noise generated is small, and at voltages less than 3 volts, it is considered negligible for good transistors. The preamplifier input transistors Q1 and Q2 are both operated with junction voltages of 1.5 volts. Consequently, this reduces the leakage noise to a minimum. The surface noise is also reduced by operating the transistor in the low current mode of microamperes.

Above approximately 1kc, the shot noise predominates. In general, this noise is the combination of the thermal noise generated by the ohmic resistances in the device, as well as the currents across the junctions. Flicker noise can be considerably reduced by proper surface treatment by the transistor manufacturer, while little improvement can be made in the magnitude of shot noise.

At higher frequencies, the noise figure of transistors increases at approximately 6 d.b. per octave for frequencies higher than $f \propto \sqrt{1 - \alpha^2}$ where $f \propto$ is the α cut-off frequency and α_0

is the low frequency current multiplication factor. This noise parameter has been reduced by employing high frequency cut-off filters in both the preamplifier and resolution amplifier.

The application of the preamplifier places a demand upon its performance in terms of the following parameters.

1. Good long term stability.
2. Low internal noise.
3. High common mode rejection.
4. High amplification factor.

The above parameters are of prime importance for maintaining high reliability during changes in ambient temperature, power supply voltage variations and external noise transients. The first and second subjects were covered earlier in this report; consequently the third requirement of common mode rejection will now be considered.

The differential amplifier design has additional features of providing two isolated input terminals. This is useful in providing an output proportional to the small difference between two large input signals. The ability of the amplifier to perform this function and reject a signal that is common to both its input terminals is known as the quantity "common mode rejection". Since there are more than one direct coupled differential stages, the voltage translation is much simpler by designing the second stage

from a complementary type of transistor. The input transistors are NPN while the second stage devices are PNP.

The imbalance between the input transistors and components will be attenuated by the common mode rejection of the input circuits of the complementary second stage. The common mode rejection CMR is primarily accomplished at the input transistor stages Q1 and Q2. The definition for the CMR parameter is given as the ratio of the magnitude of the smaller input signal to the magnitude of the output signal. The common mode rejection capability is highly dependent upon the VBE of the input transistors. The CMR capability is derived as follows:

If the expression $(\Delta V_{BE} + \Delta R_S I_{CO}) - \frac{V_{EE}}{2R_{EE}} \left(R_{E1} - R_{E2} + \frac{R_{S1}}{h_{FE1}} - \frac{R_{S2}}{h_{FE2}} \right)$

is adjusted to zero, the differential output is

$$(e_{o1} - e_{o2}) = \frac{R_L}{R_{EE}} \left[2(e_2 - e_1) \left(\frac{1 + G_2}{G_1 + G_2} \right) + e_2 \left(\frac{G_1 - G_2}{G_1 + G_2} \right) \right]$$

where

$$G_1 = \frac{R_{EE}}{R_{E1} + \frac{R_{S1}}{h_{FE1}}} \quad \text{AND} \quad G_2 = \frac{R_{EE}}{R_{E2} + \frac{R_{S2}}{h_{FE2}}}$$

The differential gain

$$G_d = \frac{2R_L}{\frac{R_{S2}}{h_{FE2}} + \frac{R_{S1}}{h_{FE1}} + R_{EE}}$$

while the common mode rejection capability is

$$CMR \geq \frac{V_{BE}}{\Delta V_{BE} + \Delta R_S I_{CO}}$$

The common mode rejection then becomes the ratio of the differential gain to the common mode gain

$$CMR = \frac{2(1 + G_2)}{G_1 + G_2}$$

The last of the four parameters required for high performance of the read amplifier system is the high amplification requirement. If the gain characteristics h_{FE} of the input transistors are relatively high with low collector currents, the overall amplification of the preamplifier will be high and the signal-to-noise ratio will be optimum.

Included in the amplifier design are two negative feedback loops. The d.c. loops are taken from the collector of transistors Q5 and Q6 via resistors R5 and R4 to the base of the input transistors Q1 and Q2. The a.c. feedback loop is composed of capacitor C1 and resistor R2 network. This frequency network is connected between the collector and base of both transistors Q1 and Q2. The purpose of this circuit is to correct for phase shift in the input stages that can be caused by the capacitive effect of the coaxial shield of the input cable.

The shot noise effect is reduced by the capacitor C3 and is effective at frequencies above 1kc. Additional high frequency roll-off is accomplished in the design of the resolution amplifier. The output impedance of the preamplifier is very low, since it is required to drive a coaxial transmission line. This is accomplished by the two emitter follower transistors Q7 and Q8.

Resolution Amplifier

The resolution amplifier, Figure 3, reduces the differentiated signal from the preamplifier to single ended operation. The two balanced outputs are added together in phase at the collector of transistor Q9. This was so designed as to provide for maximum common mode rejection in the overall system. Provisions for optimizing the CMR parameter are made by adjusting the series potentiometer R6 in the emitter of Q9. The CMR control varies the degenerative feedback of this amplifier stage. This in turn changes the amplitude of the unwanted signal and appears out of phase with the other side of the push-pull single ended stage. The end result is that it becomes canceled in the output. The difference signal, however, as referred to the input of the preamplifier, will be additive, while the extraneous interference transients that are common to both inputs will be canceled.

The bias operating voltages are stabilized throughout this section and all others by using separate zener regulator diodes. The zener diode is also used for coupling applications. This design technique permits greater flexibility in d.c. amplifier circuits that are otherwise quite limited in signal handling capabilities.

The resolution amplifier also incorporates complementary transistors for supplying the maximum gain characteristics with good stability. The complementary stage combinations are the first,

second and third transistors, Q9, Q10, and Q11. To further stabilize this section, there are four d.c. negative feedback loops and one a.c. positive feedback network. The resistor R8 is connected between the first two complementary stages Q9 and Q10. This network supplies both a negative d.c. and a positive a.c. loop.

The remaining loop currents operate in a series mode through resistors R11, R7, R12, R15, and R13 in parallel with a thermistor T1. The output transistor Q13 is further stabilized by employing the thermistor T2 in series with the emitter circuit. The overall gain of this section and the preamplifier is in the neighborhood of 30,000 times. The output of this section is connected to the input of Q14 of the phase-inverter section, Figure 4.

The resolution amplifier also includes two high frequency cut-off networks. The capacitor values for C4 and C5 of Figure 3 are designed in conjunction with the output impedance h_{22} of transistors Q10 and Q11, and the input impedance h_{11} of Q11 and Q12. The total time constant includes the capacitive reactance X_c and the equivalent resistance R_{eq} . The expression of the equivalent resistance in series with capacitor C4 is given as follows:

$$R_{eq} = \frac{1}{\frac{1}{h_{11}Q_{11}} + \frac{1}{h_{22}Q_{10}} + \frac{1}{R_L Q_{10}}} \text{ and the}$$

expression of the equivalent resistance to be used with capacitor C5 is

$$R_{eq.} = \frac{1}{\frac{1}{h_{11}Q_{12}} + \frac{1}{h_{22}Q_{11}} + \frac{1}{R_LQ_{11}}}$$

The isolation and coupling resistors would be included in the h_{11} parameters. The negative feedback resistors are high in value and therefore can be omitted in the computation.

Phase-Inverter Amplifier

The next module function covers the phase inverter amplifier. The major function of this section is to convert the negative polarity waveform into a positive and then mix it with the original positive side of the signal. The output then is all positive polarity signals for triggering the one shot multivibrator.

The paraphase amplifier and mixer stages are Q17, Q18, Q19 and Q20 of Figure 4. This circuit is also temperature compensated by using the forward characteristics of silicon diodes. The idea here is to match the forward thermal characteristic of the two silicon mixing transistors Q19 and Q20. If we consider the basic input network of transistor Q20, an equivalent L pad is formed. This includes the series resistor of R24 and the shunt resistance of h_{11} of Q20 and diodes CR10 and CR11 with resistor R21B. As the temperature rises the V_{BE} of Q20 decreases since the junction voltages vary inversely with temperature and with the resistivity of the base region. This variation is sometimes called the equilibrium barrier height. In an ideal junction, the equilibrium barrier height equals the difference of the Fermi levels in the isolated n- and p- regions of the p-n junction.

The forward thermal characteristics of the diode are the same as the transistor. Consequently, when the voltage drop across the transistor emitter to base junction decreases the two diodes CR10

and CR11 junction voltages also decrease. This causes increased current to flow through the two diodes and resistor R21B. When this occurs, the voltage drop across the series resistor R24 increases while the actual voltage at the base of transistor Q20 decreases, resulting in less current into transistor Q20 and compensation is therefore achieved for this circuit.

To further compensate for the d.c. drift that will occur in the actual phase inverter stage Q17, a cross coupled feedback system is used. Since all the stages from Q17 through to the output amplifier Q22 are again d.c. coupled, extreme care must be exercised to reduce the d.c. drift component to a minimum. The cross coupled compensation is accomplished by establishing a reference voltage between the two diodes CR10 and CR11. This voltage is controlled by the output of collector Q17 via transistor Q18. During temperature rises, the transistor Q17 collector leakage I_{CBO} times the h_{FE} current gain factor will cause the collector current to increase. This increase in current will cause a greater voltage drop across the collector load resistor. The collector voltage will then decrease and reduce the voltage reference between the two diodes CR10 and CR11. When this takes place the diode CR10 will conduct more and lower the voltage at the base of transistor Q20. This transistor will then conduct less to correct for the decrease in current of Q19 which is con-

trolled from the same voltage source at the transistor collector of Q17. The other mixer transistor Q19 is also compensated in a similar manner plus additional control from transistor Q18. Further details of this network could be expanded upon, however, due to the time element, the explanation has been reduced to a minimum.

The mixer transistors Q19 and Q20 are both used for a twofold purpose. The one already described is for mixing the two polarity signals, the other is connected with the system threshold control. It is here that the d.c. voltage is developed for operating the comparator detector section. The d.c. level of the two mixer transistor collectors is determined by the amplitude of the a.c. input signal. Consequently the d.c. voltage is the direct analog of the a.c. signal level. This provides a d.c. control voltage without rectifying the a.c. signal and adding a time constant that is normally associated with a filter. The object here is to reduce all time constants to a minimum because an error could be introduced in the overall control system. In order to further stabilize the circuitry in the inverter amplifier section, an additional feedback loop is used from the output transistor Q22 collector via resistor R33 to the two mixer transistor collectors Q19 and Q20. Second order compensation is accomplished by coupling the output from the mixer transistors to the last amplifier stage Q22 through an emitter follower Q21 and diode CR13 L pad equivalent.

lent network. This is the same technique as used in the previously mentioned drift compensation network of the mixer amplifiers.

There are two outputs from this module, one is the a.c. signal output for the switching amplifier module and the other is the d.c. threshold control voltage for the comparator detector section.

Another threshold adjustment is provided in this section. The purpose of this one is to function as a trimmer for the main control found in the comparator section. This control R32 adjusts the operating bias point for the output transistor Q22. This allows an adjustment of the a.c. signal to system noise while the other threshold control for the comparator detector is to determine the signal level at which the one shot multivibrator should fire. Consequently the signal-to-noise of the system can be adjusted separately by the control R32, while the actual level of operation (regardless of noise) can be adjusted by the comparator control R42 of Figure 6.

Switching Amplifier

The switching amplifier section, Figure 5, performs five basic functions:

1. Amplification
2. Steering
3. Gating
4. Switching
5. Converting

The first three stages Q23, Q24, and Q25 are direct coupled amplifiers. The output signal from transistor Q22 of the phase-inverter module is connected to the input of transistor Q23 via resistor R34. This resistor, as well as R35, R38 of this section, R31, R29, R28, R19, and R18 of the phase-inverter module, R9, R10, and R14 of the resolution section are all high signal level limiting resistors. This is to prevent damage to the transistor base to emitter junction at extremely high signal levels. The above mentioned limiting resistors were an added extra for increasing the reliability factor of the read system. This technique is also used throughout the entire control system.

After the first three stages Q23, Q24, and Q25, a steering diode CR16 and zener diode CR15 clipping network are employed to insure that only positive polarity signals arrived at the input of the one shot multivibrator. Double precaution is again exercised here as with the gating diode CR17, to prevent extraneous signals from

triggering the multivibrator. The gating diode CR17 is controlled by a bistable multivibrator Q36 and Q37, located in the comparator amplifier section. The bistable circuit is designed for supplying both the negative and positive d.c. control voltages to the gating diode CR17. This approach does not depend upon the normal leakage resistance of the diode. The gating diode is a high quality silicon device that exhibits very high back resistance. The circuit design, however, does not depend upon the stability of this parameter with variations in temperature. In order to insure dependable operation under all conditions, the diode CR17 is heavily reversed bias for cut-off and forward biased for the ON condition.

Capacitors C13, C14, and C15 are used as differential capacitors to insure leading edge triggering of the output signal from transistor Q25. This transistor is used as a power transfer device to supply a constant voltage to the diode networks.

The one shot multivibrator consists of transistors Q26 and Q27 which generates a pulse of constant amplitude and time duration. The positive pulse output of transistor Q27 is connected to the emitter follower transistor Q29. From here it is a.c.-coupled to the logic networks throughout the control system as well as to the converter amplifier Q30 and its associated frequency sensitive network. This network drives a small sensitive meter for monitor-

ing the frequency rate of the output pulses. The emitter follower stage Q28 provides a negative polarity pulse to a logic indicator lamp network.

Comparator Amplifier

The comparator amplifier is shown in Figure 6. This section is the key to accuracy as far as voltage detection is concerned. It is this circuit function that enables the system threshold dead zone to be reduced by an order of magnitude. This approach was considered because of its inherent high resolution in discriminating between small magnitudes of d.c. voltages. This circuit can differentiate between d.c. voltages of 5 millivolts.

The control voltage for this section is taken from the mixer transistors Q19 and Q20 of the phase-inverter amplifier. Since the d.c. voltage at this point is a direct analog of the a.c. signal level, it is used as a reference voltage for operating the system threshold control section.

Using the comparator detector approach, the system dead zone is reduced to .5 microvolts as referred to the input. The operation of this section includes a d.c. differential amplifier that controls two relaxation oscillators. The differential amplifier consists of transistors Q32 and Q35 with a reference voltage at the base of Q35 through a zener diode CR21. The two relaxation oscillators employ unijunction transistors Q33 and Q34. When no signal is present from the read velocity head, the unijunction transistor Q33 is operating. A series of high frequency pulses of very short time durations are generated and coupled through a

transformer T1 to the bistable multivibrator transistor Q37. Since the pulses are negative, the transistor Q37 is cut-off and a positive d.c. level is supplied from the collector to the cathode side of the diode gate CR17. By the same token, transistor Q36 is in the saturated mode and the collector voltage of this transistor is negative. Since this output is connected to the anode side of the diode gate, the combination of this control voltage and the one from transistor collector Q37 causes the diode to be reversed biased. The diode is now in the OFF mode and will not permit signals to pass through.

When the a.c. signal level rises above the threshold level (as set by control R42) the unijunction transistor Q33 turns off. Now an output signal from transformer T2 is present, this causes transistor Q36 to turn off and the bistable multivibrator has changed its mode of operation. Now the diode gate is biased in the forward or ON state.

The application of the bistable multivibrator in this circuit is for the purpose of filtering out the negative pulses generated by the relaxation oscillators. If conventional techniques were used, components such as rectifiers and capacitors would be required to supply the d.c. level to the diode gate. This, however, would introduce a time constant since it requires a certain period for charging and discharging the capacitors. With the bistable multi-

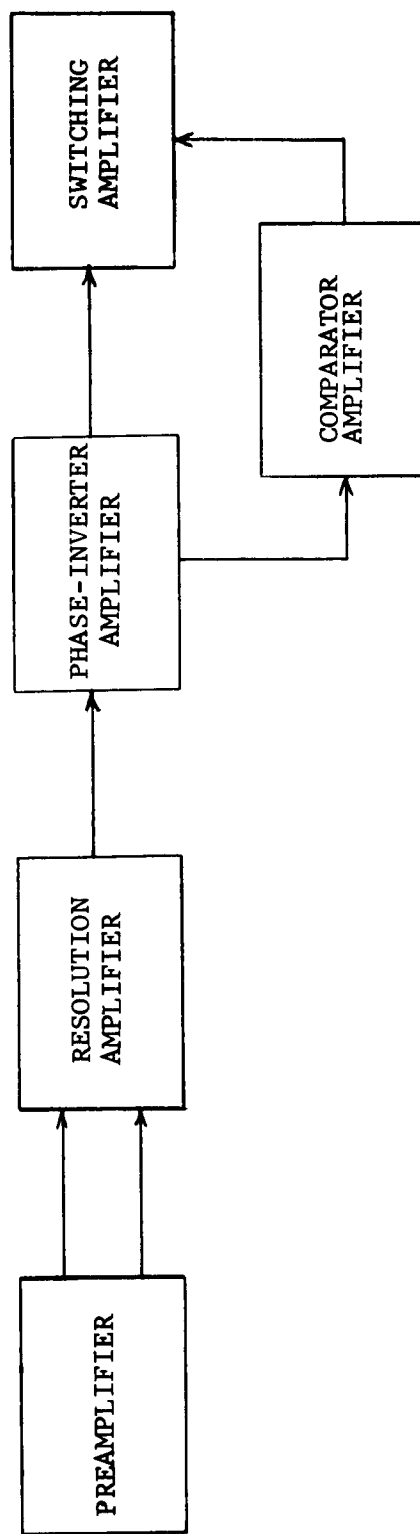
vibrator we can accomplish the same function but with a very short or no time constant, hence a solid state filter exists with microsecond response. In order to insure maximum isolation of the negative pulses from the relaxation oscillators to the diode gate and one shot multivibrator, a T network is placed in series between the bistable collector circuit and the diode gate. This network consists of resistors R44, R37 and capacitor C16 on one side, while the other network includes resistors R43, R36, and capacitor C17. The time constant of the T network is quite short, therefore, there are no degraded effects to the system response. The total switching time of the diode gate and comparator circuit is in the microsecond region.

This now concludes the technical discussion of the read amplifier which has a linear gain of approximately four million times. It is believed that the design parameters were carefully selected to insure the maximum reliability of this equipment, and that every possible attempt has been made to employ the latest state of the art techniques.

Some of the circuit functions in the read system have been either omitted or simplified. Complete circuit description will be given later in the final report.

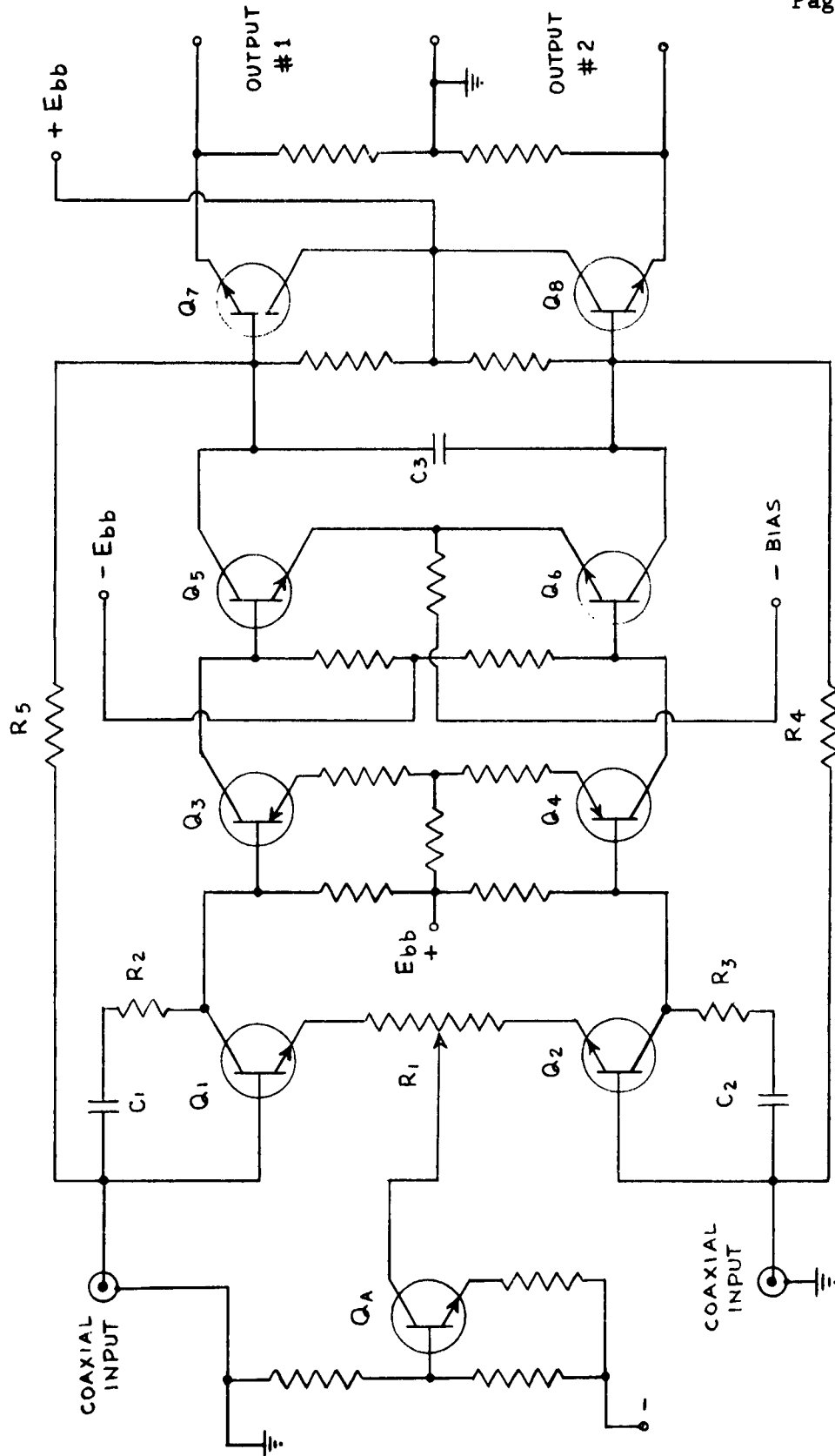
Acknowledgments and references:

- 1) The Fairchild, Philco and Sperry semiconductor companies.
- 2) The Mathematics of Circuit Analysis, John Wiley and Sons, Inc.

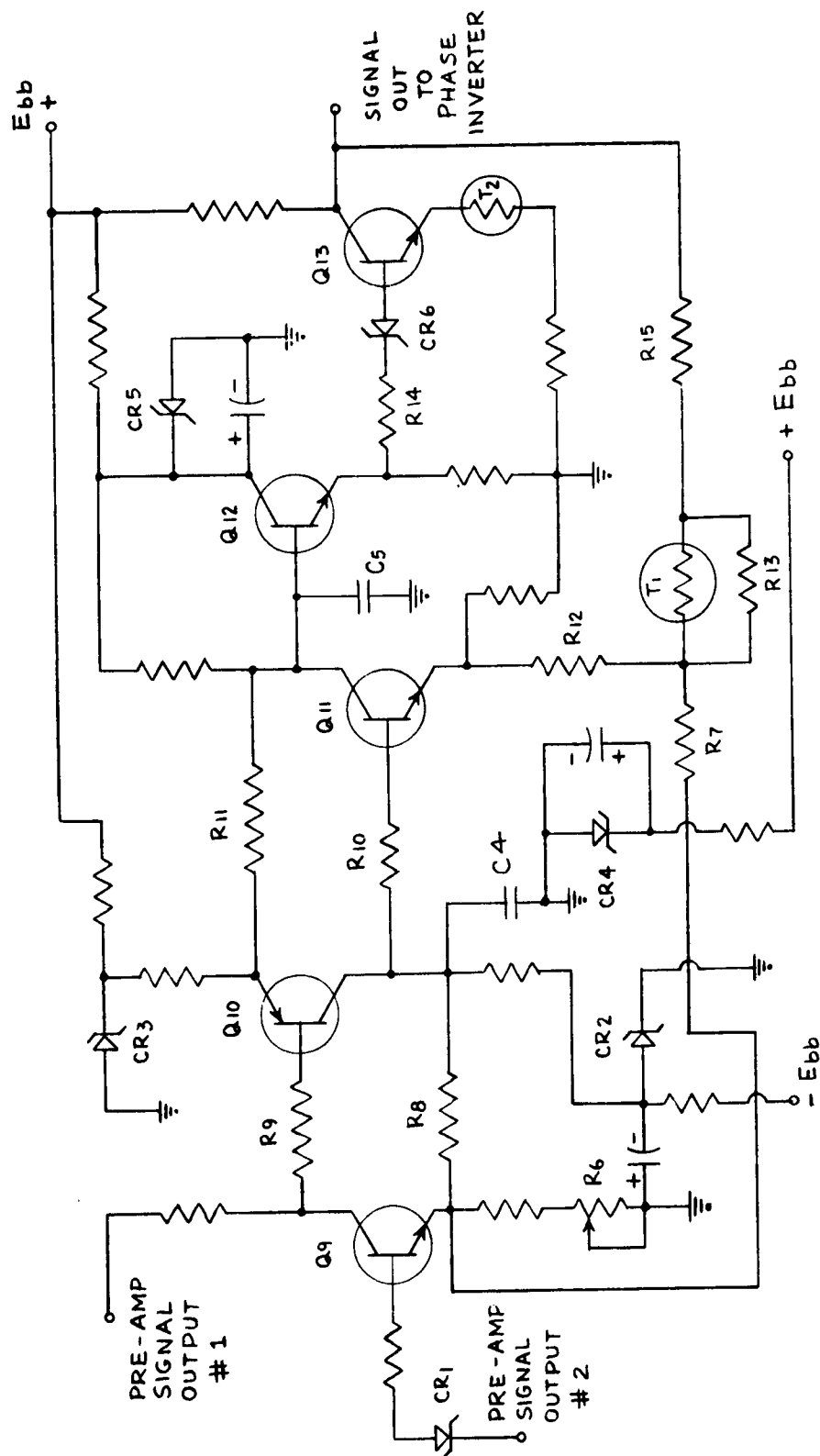


READ AMPLIFIER BLOCK DIAGRAM

FIGURE 1

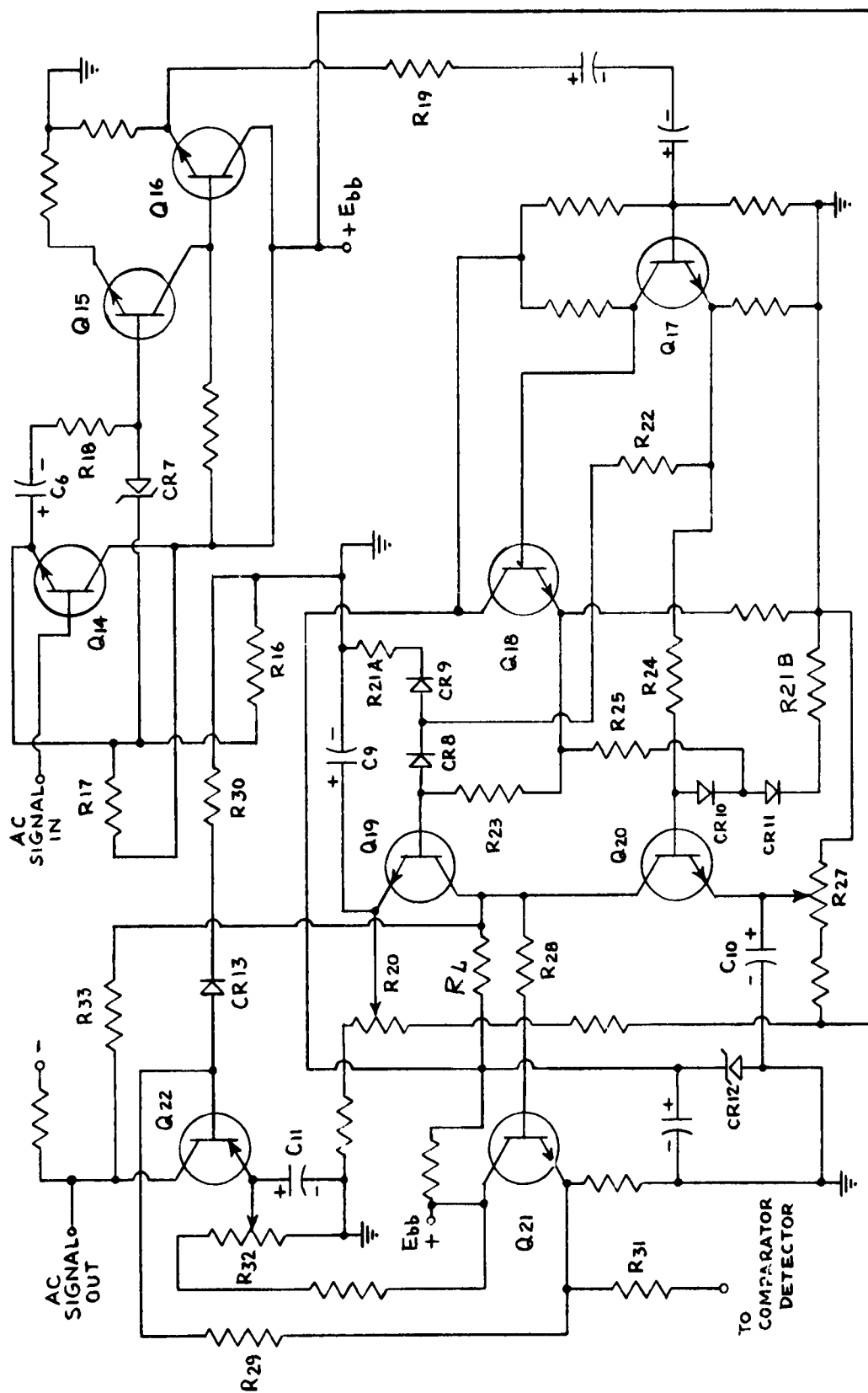


PREAMPLIFIER
FIGURE 2



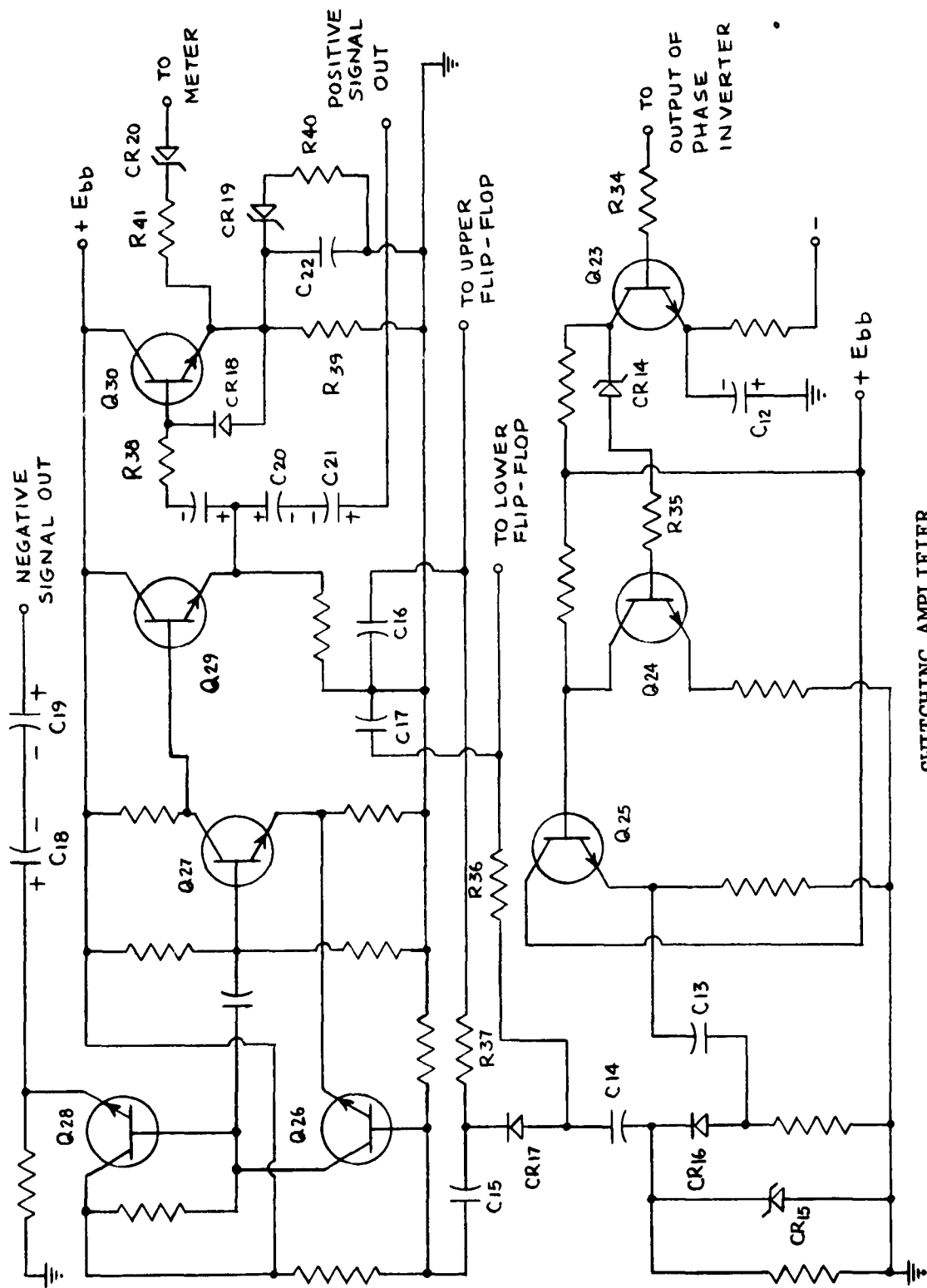
RESOLUTION AMPLIFIER

FIGURE 3



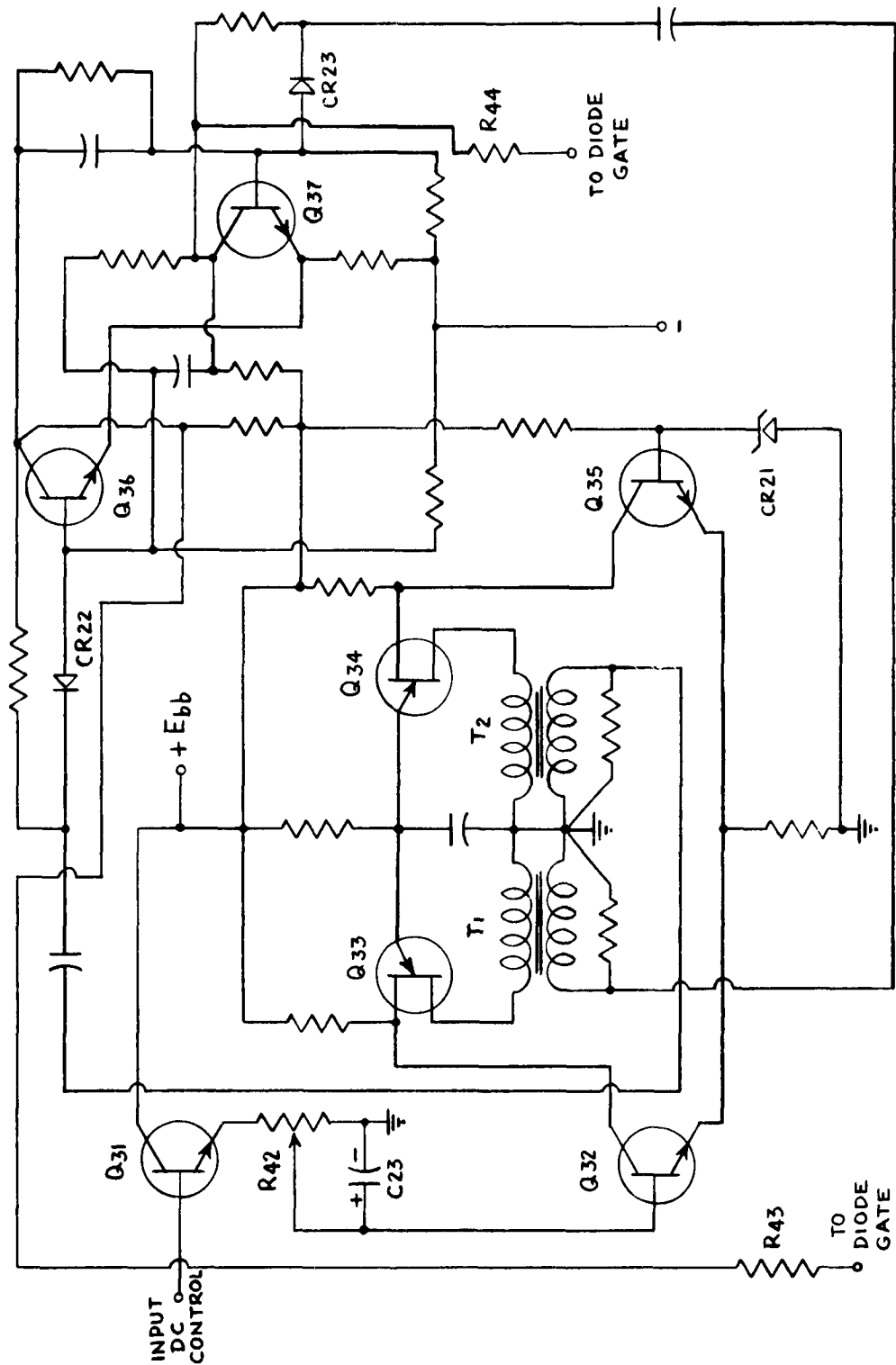
PHASE-INVERTER AMPLIFIER

FIGURE 4



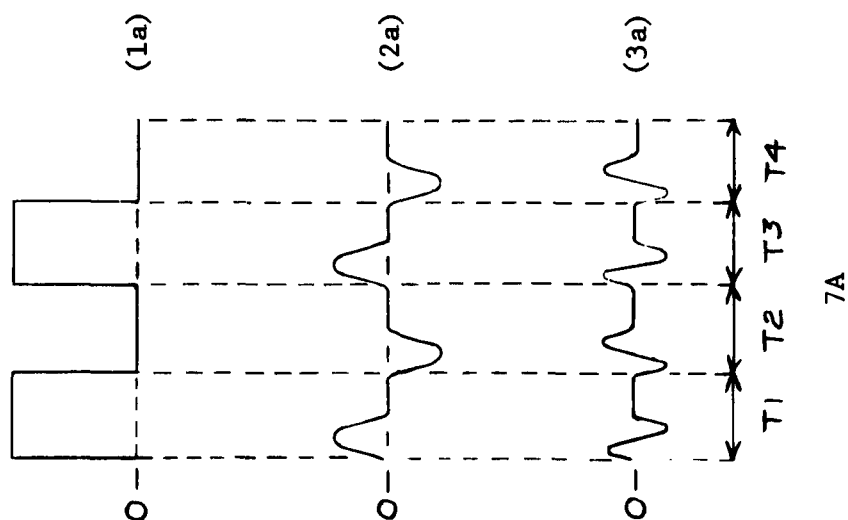
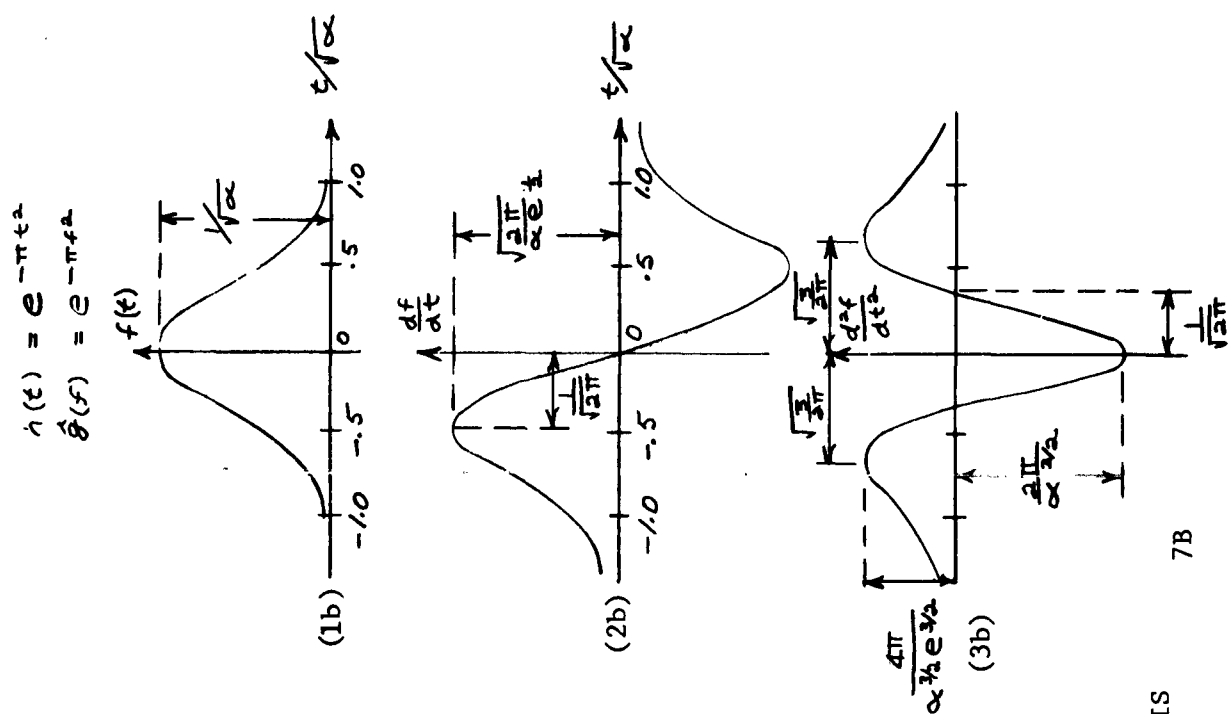
SWITCHING AMPLIFIER

FIGURE 5



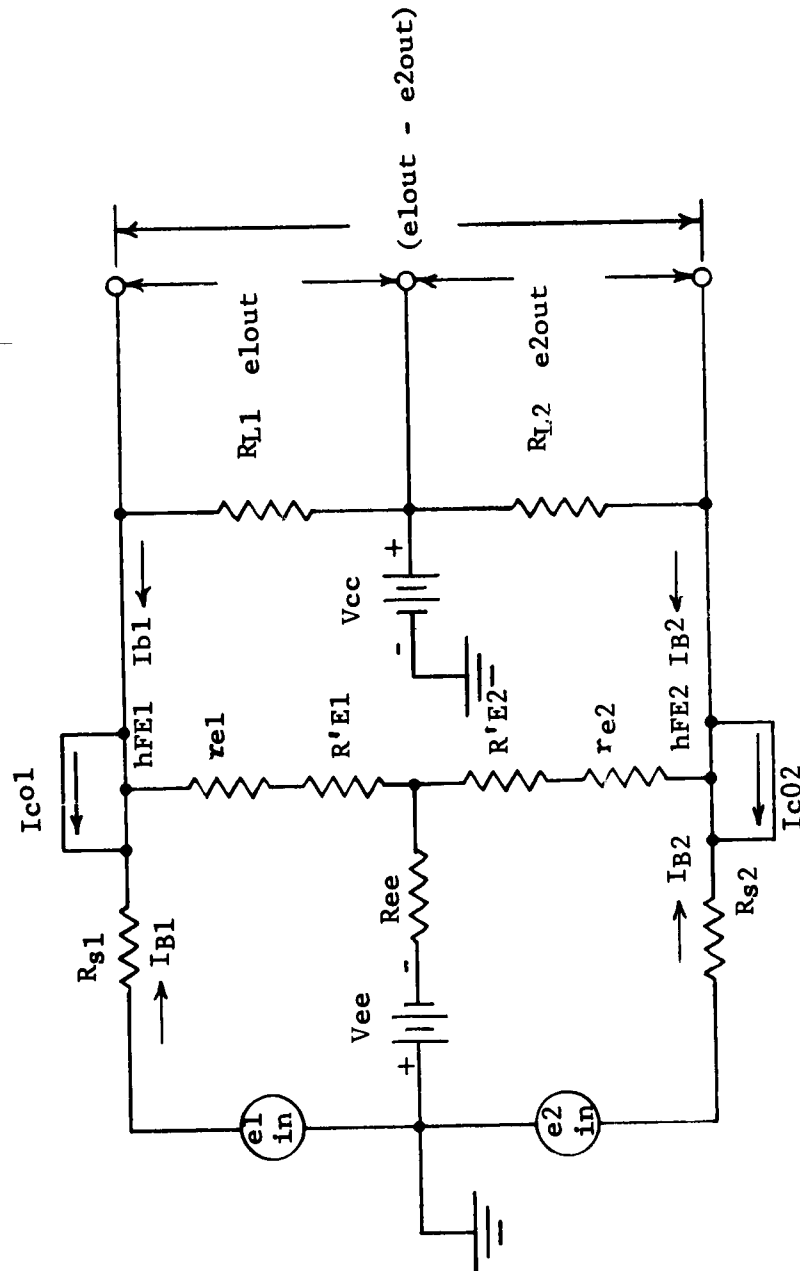
COMPARATOR AMPLIFIER

FIGURE 6



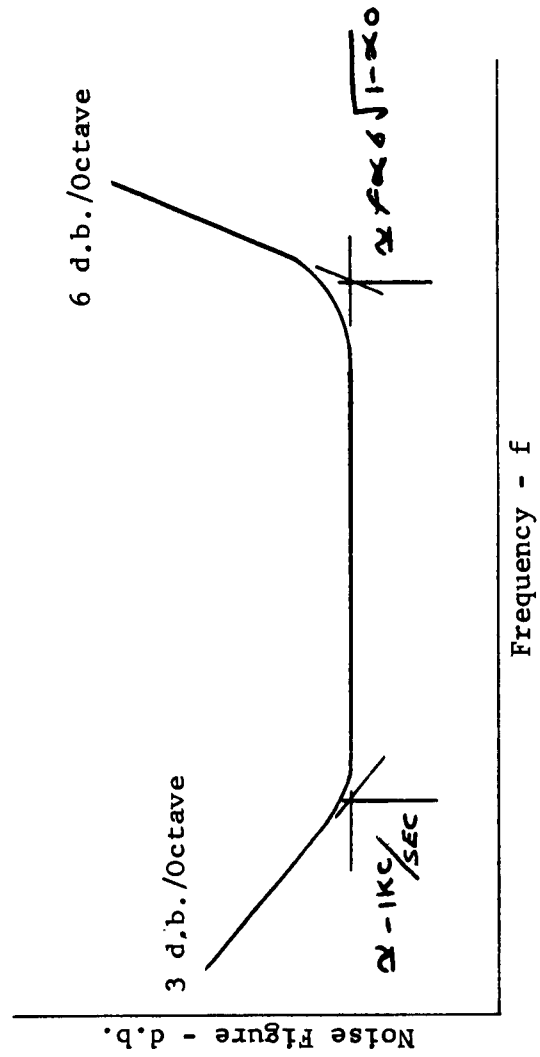
WAVFORM ANALYSIS

FIGURE 7



DIFFERENTIAL TRANSISTOR EQUIVALENT CIRCUIT

FIGURE 8



NOISE SPECTRUM FOR A TYPICAL TRANSISTOR

FIGURE 9

LENS DESIGN

During the past month major attention within Bell & Howell has been concentrated on the machine fabrication which has been fully described in earlier pages. No specific attention has been paid to the design of the 48" f/4 lens, however, because major work has been done on the Bell & Howell-sponsored project of developing a system of automatic lens design which will include the design of lenses having aspheric surfaces. This project has been under way for about six years now and has reached a stage where there is every indication that the design philosophy and the computing techniques will result in a high speed method of designing a lens such as the 48" f/4. This lens has, in fact, been used as a test problem for the automatic design procedure. This work has shown that the monochromatic aberrations can be brought under very precise control. The outstanding aberrations are secondary spectrum and sphero-chromatism. Of these the sphero-chromatism is the dominant aberration and steps must be taken to reduce it.

During the coming month the automatic design program will be applied to variations of triplet designs with a view to securing in a very short time the optimum design which this configuration is capable of giving. However, it is probable that it will be necessary to split up one of the elements of the triplet in order to produce a four element triplet. The results which may be achieved by this splitting up will be determined by using the automatic design pro-

gram, and the advantages which accrue from the extra element will be evaluated. It is possible at this time that a request then may be made at Wright Field for the substitution of a four element triplet for a three element triplet.

RECOMMENDATIONS

It is believed that during the ensuing three months, following the period covered by this report, the entire numerical control system will be integrated with the machine tool and that experiments will have progressed to the point whereby programmed glass surface contouring can begin. All areas of the control system will be tested and verified for function and reliability, section by section, before an attempt at programmed contouring is first tried.

An example of this procedure is as follows: A simple spherical contour will be programmed into the computer from which a punched tape output will be obtained. A secondary program will be processed through the computer which will give the exact number of B pulses required for the contour program. Then the programmed tape will be fed into the translator while the translator output pulses are counted electronically and checked against the computed number of pulses, representing the B pulses, called for in the program.

Once this operation proves to be reliable, the operation will be repeated with the translator output pulses fed simultaneously to the counter and the B drum on the machine tool. Then the B pulses from the drum will be read out and counted for equality with the input pulses. Before the B drum has been programmed, the A drum pulses would have been checked at the output of the read head. Next, several trial runs will be made bringing the bi-directional counter

into use whereby the C pulses, or response pulses, count down the B pulses which are the command pulses.

The design of the control system is such that each separate function can be checked digitally and, where applicable, can be double-checked by measurement of discrete linear distances or angles of travel. When the functions of all areas of the control system have proven to be reliable and repeatable, the first piece of glass will be machined from a known command tape which has been programmed by the computer and pre-checked for accuracy. Any deviations from a true sphere as measured by various means will indicate any further corrective measures to be required. Once any such corrective measures are accomplished, more complicated contours will be processed including reversals in slope, deviations from a sphere, and will finally lead to the aspheric figures called for by this contract.

DISTRIBUTION LISTNo. of Copies

Armed Services Technical Information Agency
Attn: Document Service Center (TIPSCP)
Arlington Hall Station
Arlington 12, Virginia

9

Nortronics
Attn: Mr. P. H. Halderman, Gen. Supv.
Dept. 2883
222 No. Prairie Ave.
Hawthorne, Calif.

1

American Machine & Foundry Co.
Central Regional Office
333 W. First St.
Dayton 2, Ohio

1

AMC Aeronautical Systems Center
Attn: LMBMF
Wright Patterson Air Force Base, Ohio

1

Commanding General
Air Material Command
Attn: ASRCTF/W. Webster
Wright Patterson Air Force Base, Ohio

2

Commander
Wright Air Development Division
Attn: WWRNRD-1
Wright Patterson Air Force Base, Ohio

5 and Repro..

Commander
Air Research & Development Center
Attn: RDTDEG, Mr. C. W. Kniffin
Baltimore, Maryland

1

Perkin-Elmer Corp.
Danbury Road
Norwalk, Conn.

1

Commanding General
Frankford Arsenal
Attn: ORDEA, 5500
Philadelphia 37, Penna.

1

DISTRIBUTION LIST

No. of Copies

Mr. Amrom H. Katz
Rand Corporation
1700 Main St.
Santa Monica, Calif.

1

Itek Corporation
Attn: Dr. Wm. Brower
700 Commonwealth
Boston, Mass.

1

The Bendix Corporation
Attn: Mr. Roy M. Nelson
P. O. Box 5115
Detroit 35, Mich.

1

Concord Control, Inc.
Attn: Mr. H. P. Grossimon
1282 Soldiers Field Road
Boston 35, Mass.

1

The Maico Co., Inc.
Attn: Mr. R. A. Carlson
Maico Building
Minneapolis, Minn.

1

Micro-Path, Inc.
Attn: Mr. F. T. John
5221 W. 102nd St.
Los Angeles 45, Calif.

1

DeVlieg Machine Co.
Attn: Mr. C. R. DeVlieg
450 Fair Ave.
Ferndale, Detroit 20, Mich.

1

Ex-Cell-O Corporation
Attn: Mr. G. D. Stewart
1200 Oakland Blvd.
Detroit 32, Mich.

1

The Heald Machine Co.
Attn: Mr. C. G. Menard
10 New Bond St.
Worcester 6, Mass.

1

DISTRIBUTION LIST

No. of Copies

Kearney & Trecker Corporation Attn: Mr. W. C. Beverung 6784 W. National Ave. Milwaukee 14, Wisc.	1
American Cystoscope Makers, Inc. Attn: Mr. J. H. Hett 8 Pelham Parkway Pelham Manor, New York	1
Convair Div. General Dynamics Corporation Attn: Mr. M. D. Weisinger Chief, AMR and Process Development P. O. Box 1950, Mail Zone 23-10 San Diego 12, Calif.	1
Boeing Airplane Co. Aerospace Division P. O. Box 3707 Attn: Mr. B. K. Bucey Asst. to V-Pres. Mfg. Seattle 24, Wash.	1
Douglas Aircraft Co., Inc. Attn: Mr. O. L. Rumble Tooling Mgr. 3855 Lakewood Blvd. Long Beach 8, Calif.	1
Convair Div. General Dynamics Corporation Attn: Mr. R. A. Fuhrer Chief Mfg. Engr. Fort Worth, Texas	1
Bell Aircraft Corporation Niagara Falls Airport Attn: Mr. Ralph W. Varrial Mgr. Production Engr. Buffalo 5, New York	1
The Martin Company Attn: Mr. N. M. Voorhies Baltimore 3, Maryland	1

DISTRIBUTION LIST

No. of Copies

Bendix Production Division Bendix Aviation Corporation Attn: Mr. A. J. Walsh Staff Asst. 401 Bendix Drive South Bend, Ind.	1
Boeing Airplane Co. Attn: Mr. W. W. Rutledge Mfg. Mgr. Wichita 1, Kansas	1
Goodyear Aircraft Corporation Plant G Attn: Engineering Library Akron 15, Ohio	1
Grumman Aircraft Engineering Corporation Attn: Mr. William J. Hoffman V-Pres., Mfg. Engr. Bethpage Long Island, New York	1
Hughes Aircraft Co. Attn: Mr. J. W. Moffett Chief Equipment Engr. El Segundo, Calif.	1
Lockheed Aircraft Corporation Attn: Mr. B. C. Monesmith V-Pres., Mfg. Burbank, Calif.	1
Lockheed Aircraft Corporation Georgia Division Attn: Mr. R. A. Mackenzie Mfg. Manager Marietta, Georgia	1
McDonnell Aircraft Corporation P. O. Box 516 Attn: Mr. A. F. Hartwig Chief Industrial Engr. St. Louis 66, Missouri	1

DISTRIBUTION LIST

No. of Copies

North American Aviation, Inc.
International Airport
Attn: Mr. Latham Pollock
Genl. Supt. Mfg.
Los Angeles 45, Calif.

1

North American Aviation, Inc.
Attn: Mr. M. E. Fisher
Supt. Mfg. Develop.
4300 E. 5th Ave.
Columbus 16, Ohio

1

Northrop Corporation
Norair Division
Attn: Mr. R. R. Nolan
V-Pres. & Division Mgr.
1001 E. Broadway
Hawthorne, Calif.

1

Rohr Aircraft Corporation
Attn: Mr. B. F. Raynes
Executive V-Pres.
P. O. Box 878
Chula Vista, Calif.

1

Ryan Aeronautical Co.
Attn: Mr. Robert L. Clark
Works Manager
P. O. Box 311
Lindberg Field
San Diego 12, Calif.

1

Thompson-Ramo-Wooldridge, Inc.
Attn: Mr. Carl W. Goldbeck
Asst. Staff Director Ind. Engr.
23555 Euclid Ave.
Cleveland 17, Ohio

1

Marquardt Aircraft Corporation
Attn: Mr. J. L. Liefeld
Director of Mfg.
16555 Saticoy St.
Van Nuys, Calif.

1

DISTRIBUTION LIST

No. of Copies

Massachusetts Institute of Technology
Electronic Systems Laboratory
Attn: Mr. J. E. Ward
Cambridge 39, Mass.

1

Machine Tool Automation, Inc.
Attn: Mr. G. Wolff, Chief Engr.
P. O. Box 176
Southport, Conn.

1

Sundstrand Machine Tool
Attn: Mr. Richard Leber
Belvidere, Illinois

1

Minneapolis-Honeywell Regulator Co.
Attn: Mr. D. L. Curtner
Aeronautical Div.
2600 Ridgway Road
Minneapolis, Minn.

1

AMC Ballistic Missiles Center
Attn: LBPR (Mr. F. Becker)
AF Unit Post Office
Los Angeles 45, Calif.

1

Commanding Officer
Ordnance Materials Research Office
Watertown Arsenal
Attn: N. L. Reed
Asst. Dir.
Watertown 72, Mass.

1

Director
Naval Research Laboratories
Attn: Code 2021
Washington 25, D. C.

1

Ratheon Co.
Spencer Laboratory
Attn: Mr. A. Phillips
Wayside Ave.
Burlington, Mass.

1

DISTRIBUTION LIST

No. of Copies

Defense Metals Information Center
Battelle Memorial Institute
Attn: Mr. F. Boulger
505 King Ave.
Columbus 1, Ohio

1

Professor Orlan W. Boston
1645 Arbordale Drive
Ann Arbor, Mich.

1

Mr. Julian Glasser
Staff Consultant
Materials Advisory Board
2101 Constitution Ave.
Washington 25, D. C.

1

Boeing Airplane Co.
Attn: Mr. L. Pickrell
Mfg. Development
P. O. Box 3707
Seattle 24, Wash.

1

Goodman Manufacturing Co.
Attn: Mr. Ken Stalker
Technical Director
48th Place & Halsted St.
Chicago, Illinois

1

The Norton Co.
Attn: Dr. L. P. Tarasov
Research & Development Dept.
Worcester 6, Mass.

1

Cincinnati Milling Machine Co.
Attn: Dr. M. Eugene Merchant
Director of Physical Research
4701-4801 Marburg Ave.
Cincinnati 9, Ohio

1

Republic Aviation Corporation
Attn: Mr. A. Kastelowitz
Dir. Mfg. Research
Farmingdale,
Long Island, New York

1

DISTRIBUTION LISTNo. of Copies

Shoron Optical Company, Inc.
Division of Textron, Inc.
Attn: Mr. Paul E. Dittman
Rochester 1, New York

1

Revere Camera Company
Attn: Mr. Fred Peller
320 East 21st Street
Chicago, Illinois

1

Farrand Optical Company, Inc.
Attn: Mr. Earle E. Brown
Bronx Blvd. and E. 238th St.
New York 70, New York

1

Wollensak Optical Company
Avenue D and Hudson Ave.
Rochester 21, New York

1

University of Rochester
Institute of Optics
Attn: Dr. Robert E. Hopkins
Rochester, New York

1

General Scientific Corp.
Attn: Mr. A. A. Strelsin
5153 W. 64th St.
Chicago 38, Illinois

1

Bausch & Lomb Optical Company
Attn: Joseph W. Taylor
626 St. Paul St.
Rochester 2, New York

1

American Optical Company
Research Center Library
14 Mechanic St.
Southbridge, Mass.

1

Eastman Kodak
343 State St.
Rochester 4, New York

1

DISTRIBUTION LIST

No. of Copies

Vanadium-Alloys Steel Co.
Attn: Dr. G. A. Roberts
V-Pres., Technology
Latrobe, Penna.

1

Minnesota Mining & Mfg. Co.
Attn: Mr. K. S. Jensen
400 McKnight Road
St. Paul 19, Minn.

1

General American Transportation Corporation
MRD Division
Attn: Library
7501 N. Natchez
Niles 48, Illinois

1

Texas Instruments, Inc.
Attn: Mr. C. O. Whittedge
Metrology Products Branch
13500 N. Central Expressway
Dallas, Texas

1

General Electric Co.
Large Jet Engine Dept.
Mfg. Engr. Research Laboratory
Attn: Mr. J. H. Crawford
Mail Drop E-72
Cincinnati 15, Ohio

1

Santa Barbara Research Center
Santa Barbara Airport
Attn: Judy Zisman
Library
Goleta, Calif.

1

DISTRIBUTION LIST

No. of Copies

The Fosdick Machine Tool Co.
Attn: Mr. C. E. Linden
Cincinnati 23, Ohio

1

Jones & Lamson Machine Co.
Attn: Mr. H. H. Whitmore
160 Clinton St.
Springfield, Vermont

1

Pratt & Whitney Co.
Attn: Mr. E. S. Belden
1100 Oakwood Ave.
Dayton 19, Ohio

1

Giddings & Lewis Machine Tool Co.
Attn: Mr. E. L. McFerren
142 Doty St.
Fond du Lac, Wisc.

1

Van Norman Machine Co.
Attn: Mr. J. E. Storm
Springfield 7, Mass.

1

Giannini Controls Corporation
Attn: Mr. A. C. Hummel
2600 Far Hills Ave.
Dayton 19, Ohio

1

Norden
11 W. Monument Ave.
Dayton 2, Ohio

1

The Austin Co.
Attn: Mr. C. L. Foster
19 Rector St.
New York 6, New York

1

DISTRIBUTION LIST

No. of Copies

Polan Industries
222 - 8th St.
Huntington, West Virginia

1

Elgeet Optical Co., Inc.
838 Smith
Rochester, New York

1

Pacific Optical Corp.
120 S. Glasgow
Inglewood, Calif.

1

C. P. Goerz American Optical Co.
461 Doughty Blvd.
Inwood 96
Long Island, New York

1

Curtis Laboratories, Inc.
2718 Griffith Park Blvd.
Los Angeles 27, Calif.

1

Commander
AMC Ballistic Missiles Center
Attn: Industrial Resources Div.
P. O. Box 262
Inglewood, Calif.

1

Dr. George R. Harrison
Massachusetts Institute of Technology
Cambridge, Mass.

1

Commander R. A. Holmes, III
PH-42
Department of the Navy
Bureau of Weapons
Washington 25, D. C.

1

Mr. Fred G. Longwell
International Business Machines Corp.
Military Products Division
Oswego, New York

1